Journal of Oceanography (2019) 75:513–524
https://doi.org/10.1007/s10872-019-00519-4

ORIGINAL ARTICLE

Individual particle analysis of marine aerosols collected during the North–South transect cruise in the Pacific Ocean and its marginal seas

Momoka Yoshizue[1] · Yoko Iwamoto[2,3] · Kouji Adachi[4] · Shungo Kato[5] · Siyi Sun[6,7] · Kazuhiko Miura[2] · Mitsuo Uematsu[6]

Received: 6 December 2018 / Revised: 9 July 2019 / Accepted: 10 July 2019 / Published online: 16 August 2019

Abstract

Sea-salt particles are major aerosol constituents in the marine boundary layer (MBL) and are chemically modified by acidic substances from anthropogenic, volcanic, and biogenic sources. When these acidic substances react with sea-salt particles, they can be easily scavenged from the MBL. This scavenging process influences the concentration of cloud condensation nuclei in the MBL. In this study, differences in chemical compositions of sea-salt particles collected over the Pacific Ocean and its marginal seas were investigated based on an individual particle analysis. The sources of the acidic substances that modified sea-salt particles were also estimated. Approximately 70% of the analyzed particles were fresh sea-salt particles. However, a sample collected near Guam was dominated by sulfates and was affected by polluted air masses that originated over the Asian continent. The aerosols collected around the Aleutian Islands included a large number of sulfates and modified sea-salt particles. Individual particle composition analyses indicate that these sea-salt particles were modified by methanesulfonic acid produced from marine biota and sulfuric acid from volcanic gas from the Kamchatka Peninsula. The gravitational deposition velocities of sulfates and modified sea-salt particles were calculated based on measured particle sizes. The results suggested that if acidic substances react with sea-salt particles, their lifetime in the atmosphere could be shortened due to dry deposition. Therefore, it is necessary to consider the scavenging effect of sea-salt particles for estimating the climate cooling effect by clouds over the ocean.

Keywords Marine atmospheric aerosol · Sea-salt · Sulfate · Volcanic gas · Dimethyl sulfide · Methanesulfonic acid

1 Introduction

Atmospheric aerosol particles play important roles in climate change because they can directly absorb and scatter solar radiation and form clouds by acting as cloud

Electronic supplementary material The online version of this article (https://doi.org/10.1007/s10872-019-00519-4) contains supplementary material, which is available to authorized users.

✉ Momoka Yoshizue
1218707@ed.tus.ac.jp

[1] Graduate School of Science, Tokyo University of Science, 1-3 Kagurazaka, Shinjuku, Tokyo 162-8601, Japan

[2] Faculty of Science Division I, Tokyo University of Science, 1-3 Kagurazaka, Shinjuku, Tokyo 162-8601, Japan

[3] Graduate School of Integrated Sciences for Life, Hiroshima University, 1-7-1, Kagamiyama, Higashi-Hiroshima, Hiroshima 739-8521, Japan

[4] Meteorological Research Institute, 1-1 Nagamine, Tsukuba, Ibaraki 305-0052, Japan

[5] Faculty of Urban Environmental Sciences, Tokyo Metropolitan University, 1-1 Minami-Osawa, Hachioji, Tokyo 192-0397, Japan

[6] Atmosphere and Ocean Research Institute, The University of Tokyo, 5-1-5 Kashiwanoha, Kashiwa, Chiba 277-8564, Japan

[7] JAPAN NUS Co., Ltd., 2-3-1 Minato Mirai, Nishi, Yokohama 220-6001, Japan

condensation nuclei. For example, sea-salt particles scatter solar radiation and contribute to the cooling of the Earth. However, our scientific understanding is not sufficient to accurately evaluate the climate impact of the atmospheric aerosols (IPCC 2013).

Sea-salt particles originate from the ocean, which covers approximately 70% of the Earth's surface and thus has a particularly strong influence on global climate. Sea-salt particles are generated from a bubble bursting process on the sea surface. The chemical compositions of sea-salt particles are modified when they react with acidic substances such as sulfuric acid (H_2SO_4), methanesulfonic acid (MSA; CH_3SO_3H), and nitric acid (HNO_3). The reactions between sodium chloride (NaCl), which is the main component of sea-salt particles, and the acidic substances are shown by the following chemical equations (Eqs. 1, 2, and 3).

$$2NaCl + H_2SO_4 \rightarrow Na_2SO_4 + 2HCl \uparrow \quad (1)$$

$$NaCl + HNO_3 \rightarrow NaNO_3 + HCl \uparrow \quad (2)$$

$$NaCl + CH_3SO_3H \rightarrow CH_3SO_3Na + HCl \uparrow \quad (3)$$

Major sources of H_2SO_4 are the combustion of fossil fuel, volcanic gas, and dimethyl sulfide (DMS) that originates from marine biota. HNO_3 is mainly derived from the combustion of fossil fuel. MSA is produced by the oxidation of DMS.

H_2SO_4 is a precursor of sulfates that act as cloud condensation nuclei in the marine atmosphere (e.g., Ooki et al. 2003; Berresheim et al. 1993). Hara et al. (2005) showed that when H_2SO_4 reacts with sea-salt particles, the lifetime of sulfates in the atmosphere shortens because of scavenging by sea-salt particles along coastal Antarctica. Thus, the cooling effect by clouds is largely influenced by the abundance of sea-salt particles (Gong and Barrie 2003). To understand the climate impact of sea-salt particles, it is important to investigate the extent and cause of the modification of sea-salt particles in different atmospheric environments.

Sea-salt particles modified by acidic substances have been reported in a number of studies. In urban coastal sites, some interactions between sea-salt particles and anthropogenic substances have been reported. For example, on the west coast of America, Adachi and Buseck (2015) reported that sea-salt particles were modified by H_2SO_4 or/and HNO_3, and Laskin et al. (2012) additionally reported that the surroundings of sea-salt particles were modified by organic acid. Li et al. (2011) also observed the sea-salt particles similar to those reported in Laskin et al. (2012) in Macao. In the open ocean sites, Mouri et al. (1996) and Miura et al. (1991) reported the presence of sea-salt particles modified by H_2SO_4 and HNO_3 near Japan and Indonesia. Mouri et al. (1999) reported the presence of sea-salt particles modified by acidic gases originating from marine biota over the Arctic Ocean. Chi et al. (2015) also reported the presence of sea-salt particles partially or completely modified by HNO_3 as well as by H_2SO_4 over the Arctic Ocean. Hara et al. (2005) showed that sea-salt particles were modified not only by H_2SO_4, but also by MSA in coastal Antarctica. These studies showed that the modification processes of sea-salt particles occur in various regions and causes.

In this study, we perform individual particle analyses focused on sea-salt particles collected across the globe from the Arctic Ocean to the South Pacific to understand the extent of sea-salt compositional changes over the ocean using a transmission electron microscope equipped with an energy dispersive X-ray spectrometer (TEM-EDX). In addition, the sources of the acidic substances that modify the sea-salt particles are also discussed.

2 Methods

2.1 Observation

Aerosol samples were collected onboard the R/V Hakuho Maru during the KH-13-7 cruise and the KH-14-3 Leg2 cruise in the Pacific Ocean and its marginal seas using a 3-stage impactor. Sampling was performed only when there was no contamination from the vessel itself, based on the particle number concentration and the wind direction, which were measured continuously on the vessel. The cruise tracks and the sampling points are shown in Fig. 1. In this study, 8 samples were collected among the various ocean regions: No. 1, the Arctic Ocean; No. 2, the Bering Sea; No. 3, around the Aleutian Islands; No. 4, 35°N in the trade wind belt; No. 5, around the equator; No. 6, the South Pacific; No. 7. around New Zealand; and No. 8, around Guam (Fig. 1). Five-days backward trajectories starting from 500 m above sea level (a. s. l.) at the sampling points were calculated using the NOAA Hysplit Model (http://www.ready.noaa.gov/HYSPLIT.php) (Rolph et al. 2017; Stein et al. 2015) to estimate the origins of the sampled air masses (Fig. 1). The 50% cut-off aerodynamic diameters of the impactor were 4, 0.5 and 0.25 μm with a flow rate of 1.0 $L \cdot min^{-1}$. The sampling time varied from 10 to 20 min during the KH-13-7 cruise and from 1 to 5 min during the KH-14-3 Leg2 cruise, depending on the particle number concentration. A carbon-coated nitrocellulose (collodion) film supported on a Cu grid was used for the collection substrates.

During both cruises, particle number concentrations were continuously measured using an optical particle counter (OPC; KC-01D, RION) with 5 channels in diameters greater than 0.3, 0.5, 1, 2, 5 μm. The OPC was installed in an observation box mounted in front of the upper deck and the sampled air was introduced to the box from an inlet on its ceiling. During the KH-13-7 cruise, the sampled air was dried

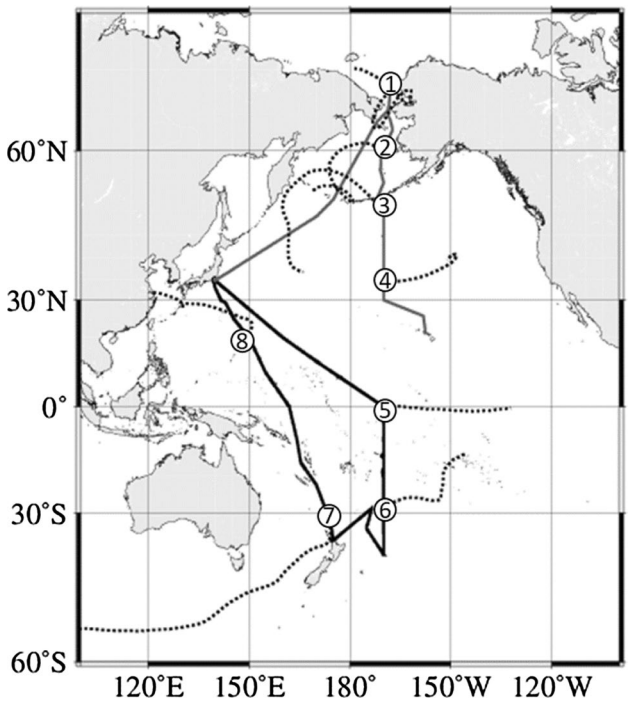

Fig. 1 Cruise tracks of the KH-13-7 cruise (black line) and the KH-14-3 Leg2 cruise (gray line). Circled numbers indicate the sampling points (①: No. 1 the Arctic Ocean, ②: No. 2 the Bering Sea, ③: No. 3 around the Aleutian Islands, ④: No. 4 35°N in the trade wind belt, ⑤: No. 5 around the equator, ⑥: No. 6 the South Pacific, ⑦: No. 7 around New Zealand, ⑧: No. 8 around Guam). The dotted lines show five-days backward trajectories starting from 500 m a. s. l. at the sampling points

prior to sampling to a relative humidity less than 30% using a diffusion dryer. The radon concentration was measured using two radon counters (the KH-13-7 cruise: ES-74230, JREC CO., Ltd.; the KH-14-3 Leg2 cruise: ES-7267, JREC CO., Ltd.). Radon is chemically inactive and decreases through radioactive decay. Since radon mainly originates from soil, radon in the atmosphere over the ocean can be used as a tracer of air masses from continents. Furthermore, a high-volume air sampler (AS-9, KIMOTO ELECTRIC CO., LTD.) collected aerosol particles on filters every 24 h. To minimize contamination from the vessel, the samples were collected only when the relative wind directions to the bow were from $-90°$ to $+90°$ and the relative wind speed was more than 1 m s^{-1}. The filter samples were analyzed using ion chromatography to measure the concentration of MSA and water-soluble ion components in the laboratory. Air samples were also collected in canisters to measure atmospheric DMS concentrations using GC-FID (GC6890, Agilent Co. Ltd.) in the laboratory.

2.2 EDX analysis

Elemental compositions of individual particles were determined using an energy dispersive X-ray spectrometer (EDX; Oxford X-MAX-80, Oxford Instruments) equipped with a transmission electron microscope (TEM; JEM-1400, JEOL). The circle equivalent diameters were measured from the particle areas obtained from the TEM image. We determined the relative masses of C, N, O, Na, Mg, Al, Si, P, S, Cl, K, Ca, Ti, Mn, Fe and Zn for individual particles using software in the EDX (INCA, Oxford Instruments). If the count rate of characteristic X-rays is less than 12.5 counts s^{-1} or the relative mass ratio of a certain element exceeds 100%, the data are excluded from the discussion due to high uncertainty (approximately 7% of all data). To verify the quantitative analysis, laboratory-generated standard NaCl particles using 0.1% NaCl solution made with NaCl of 99.5% purity (KANTO CHEMICAL CO., INC.) were measured using the EDX. Based on the result of the standard particles, particles with circle equivalent diameters larger than 0.3 μm were used for the following analysis (Text S1).

2.3 Definition of sea-salt particles

The composition of fresh sea-salt particles may be the same as that of sea water, and the relative mass ratio of Na within the main six elements (Na, Cl, S, Mg, K, Ca) of sea water is approximately 30%. However, the relative Na mass ratio commonly decreases when sea-salt particles completely deplete Cl and attach excessive S on their surfaces. Thus, in this study, according to Miura (2000), sea-salt particles are defined as those that contain more than 15% Na in the total mass.

3 Results

3.1 General descriptions of the sampling periods

During both cruises, we monitored continuously meteorological parameters and concentrations of radon and aerosol particles. Both the radon concentration and particle number concentration were the highest around Guam (No. 8) (Table 1). However, the radon concentration was low over the central part of the Pacific (No. 4–6). The DMS concentrations were relatively high over the Northern Hemisphere (No. 1–4), especially over the Arctic Ocean (No. 1) and around the Aleutian Islands (No. 3), but the concentration was below the detection limit around Guam (No. 8). The MSA concentrations were high over the Arctic Ocean (No. 1), the South Pacific (No. 6) and around Guam (No. 8), but they were below the detection limit over the central part of the Pacific (No. 4, 5). The concentration of SO_4^{2-} was

Table 1 Sampling information. Sampling periods, meteorological conditions, concentrations of particles ($d > 0.3$ μm and $d > 1.0$ μm), radon (Rn), DMS, MSA, SO_4^{2-}, non-sea-salt (nss) SO_4^{2-} and NO_3^- in the atmosphere

Sample No.	Ocean region	Time (UTC)		Wind speed ($m \cdot s^{-1}$)	Humidity (%)	Particle conc. > 0.3 μm ($\#\cdot cm^{-3}$)	Particle conc. > 1.0 μm ($\#\cdot cm^{-3}$)	Rn conc. (a.u.)	DMS conc. (pptv)	MSA conc. ($ng \cdot cm^{-3}$)	SO_4^{2-} conc. ($ng \cdot cm^{-3}$)	nss-SO_4^{2-} conc. ($ng \cdot cm^{-3}$)	NO_3^- conc. ($ng \cdot cm^{-3}$)
1	The Arctic Ocean	7/30/2014	22:36–22:39	7.1	91.1	11	2.4	514	802	203	194	194	16
2	The Bering Sea	7/29/2014	02:05–02:08	4.5	87.9	31	0.4	318	140	31	337	337	14
3	Around the Aleutian Islands	7/25/2014	22:17–22:20	6.0	91.6	15	0.7	94	416	–	–	–	–
4	35°N in the trade wind belt	7/22/2014	01:28–01:31	7.0	79.3	14	2.5	66	184	n.d.	237	175	28
5	Around the equator	12/22/2013	20:16–20:26	8.2	71.3	4.7	1.0	66	40	n.d.	348	247	32
6	The South Pacific	1/9/2014	20:12–20:27	7.2	84.9	4.2	0.9	41	53	107	216	161	17
7	Around New Zealand	1/27/2014	02:52–03:12	11.5	68.1	13	2.2	–	47	–	–	–	–
8	Around Guam	2/6/2014	03:58–04:13	5.9	57.3	89	0.9	2199	n.d.	121	2503	2429	135

Concentrations of MSA, SO_4^{2-}, nss-SO_4^{2-} and NO_3^- were measured for particles of $d < 2.5$ μm. "–" and "n.d." mean no measurement and no detection

the highest around Guam (No. 8) and was the lowest over the Arctic Ocean (No. 1). The concentration of non-sea-salt SO_4^{2-} (nss-SO_4^{2-}) was the highest around Guam (No. 8). All SO_4^{2-} was nss-SO_4^{2-} over the Arctic Ocean (No. 1) and the Bering Sea (No. 2). The concentration of NO_3^- was the highest around Guam (No.8) and was relatively low over the other ocean regions.

3.2 Classification of particles

In this study, elemental compositions, shapes and sizes of the particles collected in the middle stage (0.5 μm of 50% cut-off diameter) were analyzed. The circle equivalent diameters of the analyzed particles measured using TEM agree with the cut-off sizes (Text S2).

The analyzed particles were classified into the following categories (Text S3): "C-rich", "Sea-salt", "Modified sea-salt", "Sulfate", "Potassium salt", "Sea-salt + Mineral", "Modified sea-salt + Mineral", "Sulfate + Mineral", "Potassium salt + Mineral", "Mineral" and "Others". Figure 2 shows the number fractions of the particle classification for each sample. Sea-salt particles accounted for more than 80% and modified sea-salt particles accounted for 0–5% in the samples collected over the Arctic Ocean (No. 1), 35°N in the trade wind belt (No. 4), around the equator (No. 5), over the South Pacific (No. 6) and around New Zealand (No. 7). The samples collected over the Bering Sea (No. 2) and around the Aleutian Islands (No. 3) contained more sulfates and modified sea-salt particles than the other samples. In addition, the sample collected around Guam (No.8) contained more than 85% sulfates and approximately 12% sulfate + mineral particles. Recently, several studies pointed out that Fe-bearing particles have large impact on the global carbon cycle by effecting ocean biogeochemistry through the deposition of soluble Fe to the ocean (e.g., Furutani et al. 2011; Matsui et al. 2018). For example, Li et al. (2017) reported that Fe particles collected over the East China Sea were embedded in sulfates emitted from anthropogenic combustion and had spherical shapes and sometimes aggregated. However, Fe-containing particles accounted for only approximately 0.3% in our samples.

3.3 Cl/Na ratio

To investigate the extent of modification of sea-salt particles, we calculated the Cl/Na mass ratio (Cl/Na ratio) of sea-salt particles such as "Sea-salt", "Modified sea-salt", "Sea-salt + Mineral" and "Modified sea-salt + Mineral" (Fig. 3). The median Cl/Na ratios of samples No. 2 and 4–7 agree with that of standard particles or theoretical NaCl, but those of collected over the Arctic Ocean (No. 1) and around

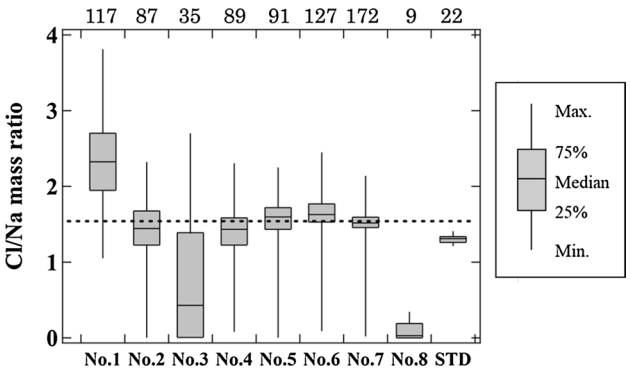

Fig. 3 Box plot of Cl/Na mass ratios for each ocean region and standard particles. Horizonal axis indicates sample numbers and STD which means standard particles. The numbers above the graph indicate the total number of "Sea-salt", "Sea-salt + Mineral", "Modified sea-salt" and "Modified sea-salt + Mineral" particles. The dashed line shows the ratio of pure NaCl (1.54)

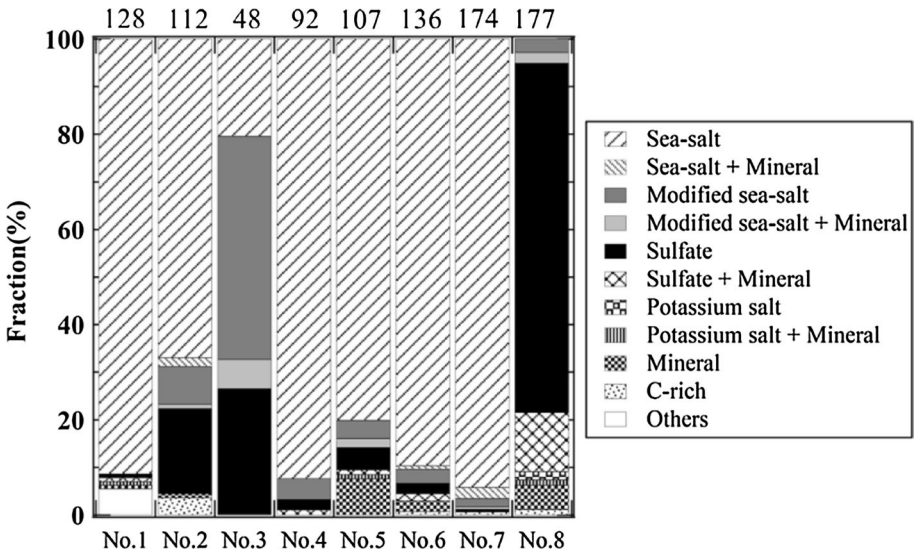

Fig. 2 Number fractions of particles for each ocean region. Horizonal axis indicates sample numbers. The values above the graph indicate the number of analyzed particles

Guam (No. 8) were, respectively, much larger and smaller than standard particles. Possible reasons for the anomalous Cl/Na ratios are discussed later. Specifically, most of the sea-salt particles collected around Guam (No. 8) were completely depleted Cl. For the sample collected around the Aleutian Islands (No. 3), the Cl/Na ratio varied widely and the modification of sea-salt particles was diverse, possibly due to the size variation of the analyzed particles (Text S2).

The relationship between Cl/Na ratios and circle equivalent diameters in Fig. 4 shows that 78% of the analyzed particles roughly agree with the Cl/Na ratio of NaCl (1.54 ± 0.5), although there are some exceptions. For example, approximately 8% of particles < 1.0 µm have small Cl/Na ratios. This trend has been reported in previous studies (Mouri and Okada 1993), which explained that (1) the smaller particles have longer lifetimes in the atmosphere and are more likely to react with acidic substances, and (2) smaller particles have larger surface-to-volume ratios. Additionally, in the sample collected around the Aleutian Islands (No. 3), some particles > 1.0 µm had small Cl/Na ratios. The reason for this is discussed in Sect. 4.2.

3.4 Sea-salt particles collected over each ocean region

To discuss the species of acidic substances that modified the sea-salt particles over each ocean region, variations in the relative mass ratio of Na, S and Cl in individual sea-salt particles are shown in Fig. 5 by reference to Hara et al. (2005). In the ternary diagrams, dashed lines and dotted lines show the stoichiometric change in chemical composition from NaCl to Na_2SO_4 and CH_3SO_3Na. Therefore, plots around dashed and dotted lines indicate the sea-salt particles modified by H_2SO_4 and MSA, respectively. When sea-salt particles are modified by other acidic substances such as HNO_3 and organic acids, they are plotted above dashed lines and it cannot be determined which acid substance modified sea-salt particles. Even if sea-salt particles do not react with MSA, those containing minerals such as Ca and Mg are plotted on dotted lines due to their relatively low proportion of Na, therefore, they are separately plotted. Sulfur dioxide is sometime taken into sea-salt particles in aqueous-phase to form S(IV) such as $NaHSO_3$, however, S(IV) is quickly oxidized to S(VI) such as Na_2SO_4 (Seinfeld and Pandis 2016). Therefore, the presence of $NaHSO_3$ is not considered.

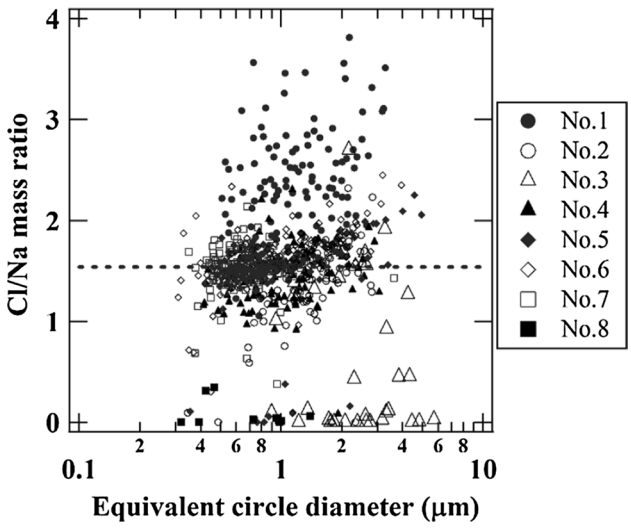

Fig. 4 Cl/Na mass ratios for individual sea-salt particles versus equivalent circle diameters. The dashed line shows Cl/Na mass ratio of pure NaCl (1.54)

There are few sea-salt particles modified by HNO_3 or organic acids over all ocean regions. The sample collected over the Arctic Ocean (No. 1) did not contain modified sea-salt particles, i.e., they were fresh, Cl-rich sea-salt particles. Only a few sea-salt particles were modified by H_2SO_4 and MSA in samples collected over the Bering Sea (No. 2), 35°N in the trade wind belt (No. 4), around the equator (No. 5), the South Pacific (No. 6) and around New Zealand (No. 7). In the sample collected around the Aleutian Islands (No. 3), some sea-salt particles were modified by MSA and some sea-salt particles were completely depleted Cl and contained excessive S. In the sample collected around Guam (No. 8), almost all sea-salt particles were completely depleted Cl. In this study, we further focused on samples that had different extents of modification of sea-salt particles collected over the Arctic Ocean (No. 1), around the Aleutian Islands (No. 3) and around Guam (No. 8).

4 Discussion

4.1 Arctic ocean

The sea-salt particles collected over the Arctic Ocean (sample No. 1) were less modified and many particles had higher Cl/Na ratios than that of sea water (Fig. 3). The high Cl/Na ratio could be caused by other chloride salts containing Mg, Ca or K, all of which are present in sea water. Hara et al. (2005) reported that sea-salt particles produced by fractionation in sea ice contain more Mg, Ca and K than sea water. The ternary diagrams in Fig. 6 suggest that the sea-salt particles include Mg, Ca and K, and specifically that they contain more Mg than sea water, consistent with results of Hara et al. (2013). The results indicate that the presence of Mg, Ca and K chloride particles increased the Cl/Na ratio in the Arctic Ocean.

Although the concentrations of atmospheric DMS and MSA were high in this sample, there were few sea-salt particles that were modified by MSA and H_2SO_4. A possible reason is that these particles were freshly emitted by a strong

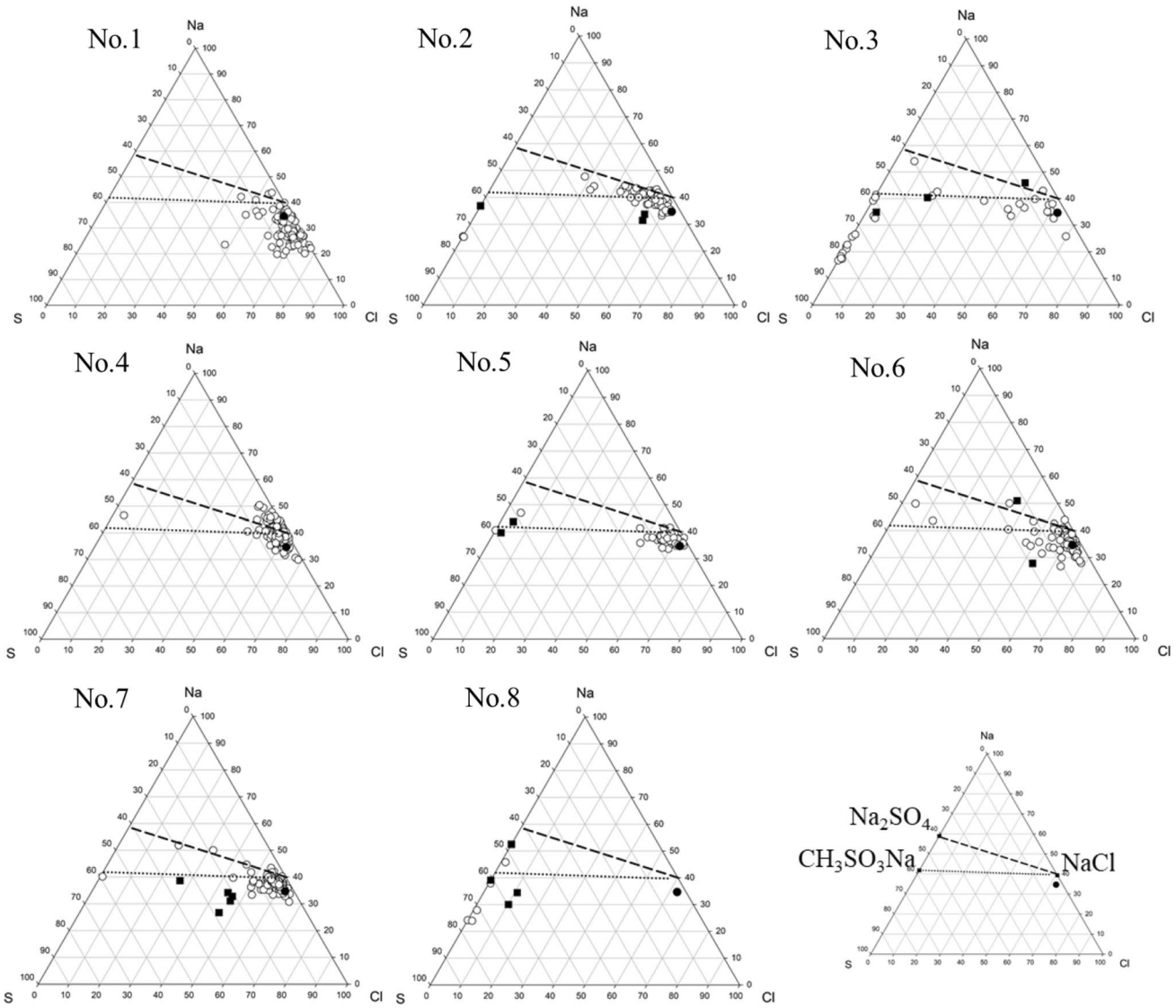

Fig. 5 The relative mass ratios of Na–S–Cl of individual sea-salt particles. Black circles show the composition of sea water. Open circles show "Sea-salt" or "Modified sea-salt" and black squares show "Sea-salt + Mineral" or "Modified sea-salt + Mineral". Dashed and dotted lines show the stoichiometric lines of NaCl–Na_2SO_4 and NaCl–CH_3SO_3Na, respectively. Plots on the dashed lines and dotted lines indicate modification by H_2SO_4 and MSA, respectively. Plots above the dashed lines indicate modification by other acidic substances

wind. The wind speed at the sampling site was 7.1 m s^{-1}, which is higher than that in other ocean regions (Table 1). When the wind speed is high, the generation of sea-salt particles from the ocean surface increases. As a result, there may be many fresh sea-salt particles that had little time to react with acidic substances over the observed area in the Arctic Ocean, resulting in many unreacted sea-salt particles.

4.2 Around the Aleutian Islands

Around the Aleutian Islands (sample No. 3), the Cl/Na ratio varied widely, and the extent of modification of sea-salt particles was variable (Fig. 3). The plots on the dotted line in Fig. 5 No. 3 indicated that approximately half of sea-salt particles were modified by MSA. On the other hand, the remaining sea-salt particles were completely depleted Cl and contained excessive S, suggesting that acidic substances other than MSA could contribute the modification of sea-salt particles. Judging from its backward trajectory (Fig. 1), the influences of anthropogenic sources on the sample were small. However, according to VOLCANO DISCOVERY (http://www.volcanodiscovery.com; accessed on November 1, 2017), the Zhupanovsky volcano (altitude: 2958 m) on the Kamchatka peninsula erupted from July 16 to 21, 2014, and the volcanic smoke reached 7 km a. s. l. on July 16. The forward trajectories starting from the Zhupanovsky volcano

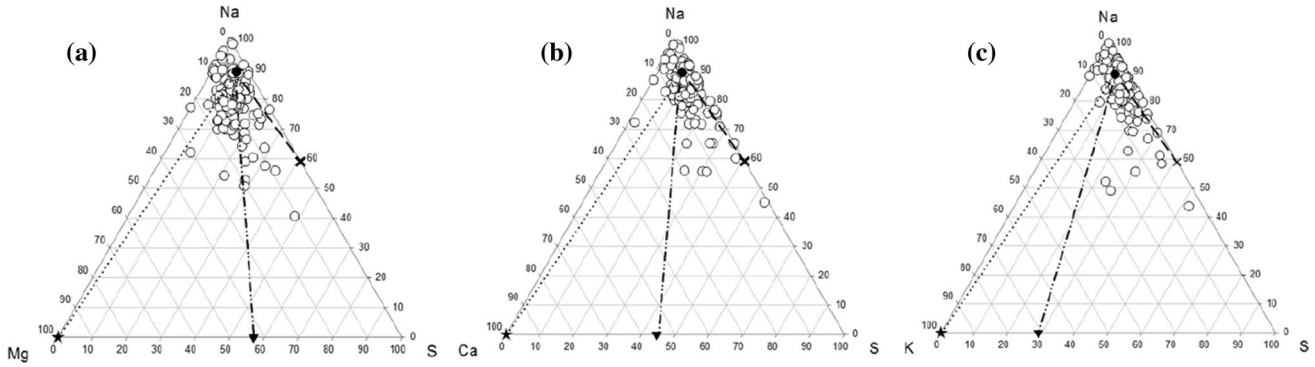

Fig. 6 The relative mass ratios of **a** Na–Mg–S, **b** Na–Ca–S, and **c** Na–K–S of individual sea-salt particles. Black circles and crosses show the compositions of sea water and Na_2SO_4, respectively. Dashed lines show the stoichiometric line of sea water-Na_2SO_4. Stars and inverted triangles show $MgCl_2$ and $MgSO_4$ in (**a**), $CaCl_2$ and $CaSO_4$ in (**b**) and KCl and K_2SO_4 in (**c**). Dotted lines and two-dot chain lines show the stoichiometric lines of sea water-$MgCl_2$ and sea water-$MgSO_4$ in (**a**), sea water-$CaCl_2$ and sea water-$CaSO_4$ in (**b**) and sea water-KCl and sea water-K_2SO_4 in (**c**)

(altitude: 3000 m) were calculated during the eruption using the NOAA Hysplit model (Fig. 7a). The forward trajectories starting at 15:00 and 16:00 on July 20 reached the sampling point on the afternoon of July 25 when the TEM sample was collected. Therefore, in addition to biogenic sulfur, H_2SO_4 from the volcano on the Kamchatka Peninsula possibly contributed to the modification of sea-salt particles.

Giant sulfates whose diameters were more than 2 µm were observed in this sample (Fig. 7b, c). Mouri et al. (1995) and Tomimatsu et al. (2012) observed similar giant sulfates in the marine atmosphere. Tomimatsu et al. (2012) showed that when a volcanic smoke reaches the free troposphere, giant sulfates can be generated by gas-to-particle conversion and coagulation during sedimentation. In this study, the backward trajectory passed through the Kamchatka Peninsula 3 days before reaching the sampling point (Fig. 1), and then its air masses came down between the marine boundary layer and the free troposphere (approximately 1500 m a. s. l.) (Fig. 7d). This trajectory suggests that the giant sulfates were generated during sedimentation. Moreover, its air masses experienced high humidity states 24 h prior to reaching the sampling point (Fig. 7d), which is a condition that possibly promotes sulfate growth (LeGrande et al. 2016).

4.3 Around Guam

The sea-salt particles collected around Guam (sample No. 8) had very low Cl/Na ratios and contained excessive S (Figs. 3, 5). In addition, sulfates accounted for more than 85% in this sample (Fig. 2). The concentrations of radon, nss-SO_4^{2-} and NO_3^- were one order higher than those of other ocean regions (Table 1). Its backward trajectory indicated the long-range transport of air masses form the Asian continent without passing near Guam island (Fig. 1). These results indicate that sea-salt particles were modified by anthropogenic H_2SO_4 in the polluted air masses derived from the Asian continent.

4.4 Deposition velocities of modified sea-salt particles and sulfates

There are few studies to calculate the deposition velocities of sulfates reacting sea-salt particles quantitatively, therefore we actually calculated them in this study. Figure 8 shows the gravitational deposition velocities V_x were calculated using their geometric mean particle sizes and densities, according to Kasten (1968). A sulfate and a modified sea-salt particle are assumed to be $H_2SO_4 \bullet H_2O$ and Na_2SO_4, respectively, and Stokes' formula (Eq. 4) was used for the calculation.

$$V_x = \frac{2}{9}\frac{(\rho_p - \rho_a)}{\mu}\left(\frac{d}{2}\right)^2 g \tag{4}$$

where ρ_p is the density of a particle ($\rho_{H_2SO_4 \cdot H_2O} = 1.79 \mathrm{g\ cm^{-3}}$, $\rho_{Na_2SO_4} = 2.66 \mathrm{g\ cm^{-3}}$), ρ_a is the density of air, μ is the viscosity of the air (U.S. Standard Atmosphere 1976) and d is the particle diameter. The mean values and the standard deviation of gravitational deposition velocities of sulfates and modified sea-salt particles were 0.16 ± 0.13 m h^{-1} and 0.81 ± 1.1 m h^{-1}, respectively. When H_2SO_4 reacts with a sea-salt particle, the gravitational deposition velocity can be approximately five times greater than when H_2SO_4 becomes a sulfate particle. This result suggests that when the acidic substances react with sea-salt particles, their lifetime in the atmosphere could shorten in terms of dry deposition.

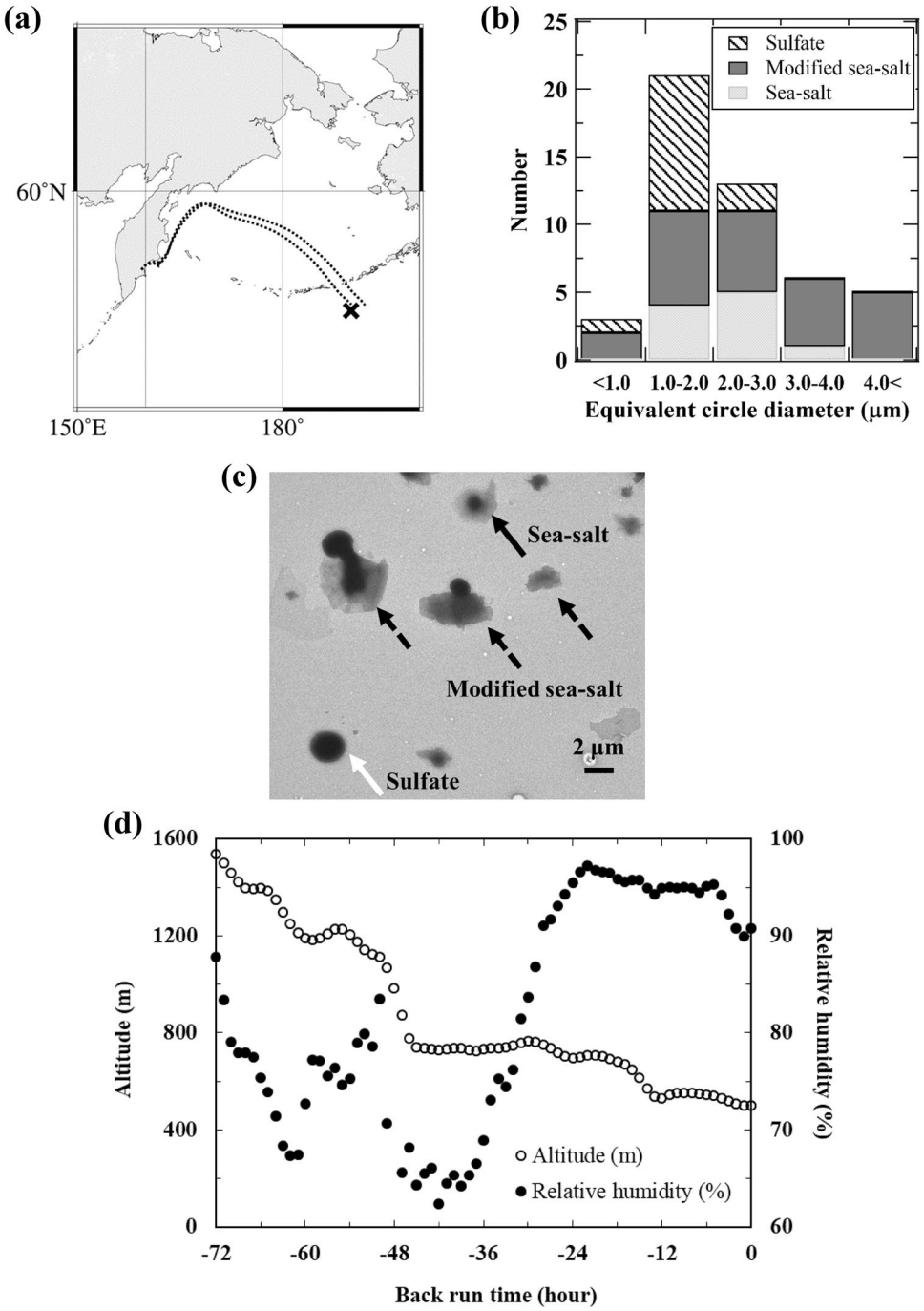

Fig. 7 **a** Five-days forward trajectories starting from the Zhupanovsky volcano (altitude: 3000 m). A cross shows the sampling point. The start times of trajectories were 16:00 and 17:00 on July 20, 2014. **b** Particle classification based on their sizes. **c** TEM image of the sample. The black, a black-dashed and white arrows indicate "Sea-salt", "Modified sea-salt" and "Sulfate", respectively. **d** Altitude and relative humidity of air masses obtained from the three-days backward trajectory

5 Conclusion

Individual particle analyses using TEM-EDX were performed on aerosol particles collected over a wide area of the Pacific Ocean and its marginal seas. The results in this study are summarized as follows.

(1) Fresh sea-salt particles accounted for approximately 80% of the constituents in the samples collected over most observed ocean regions.

(2) The sea-salt particles collected over the Arctic Ocean had greater Cl/Na mass ratios than the other samples. These sea-salt particles contained many Ca, Mg, and K chloride particles.

(3) The sample collected around the Aleutian Islands contained high sulfate and modified sea-salt particle fractions compared to the other samples. The sea-salt particles are possibly modified by MSA that formed through the oxidation of DMS that originated from marine biota

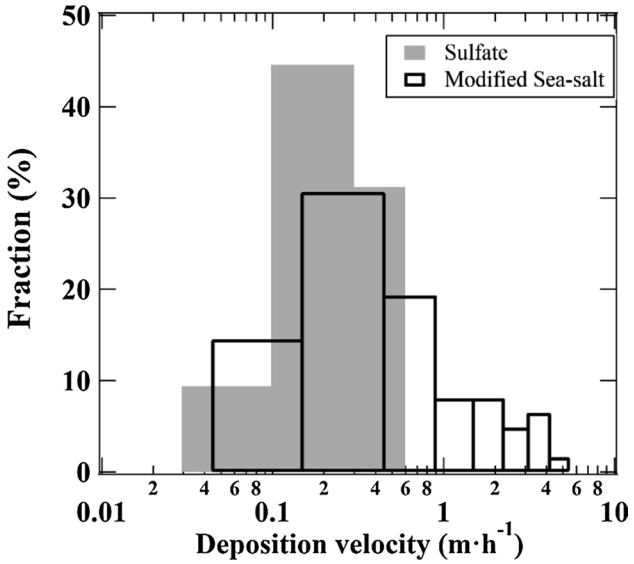

Fig. 8 Deposition velocities of $H_2SO_4 \cdot H_2O$ and Na_2SO_4. The histograms show the particle size distributions of sulfates (gray column; "Sulfate" and "Sulfate + Mineral") and modified sea-salt particles (black column; "Modified sea-salt" and "Modified sea-salt + Mineral")

and H_2SO_4 that originated from a volcanic plume that emanated from the Kamchatka Peninsula.

(4) Sulfates accounted for 85% of the sample collected around Guam. Most sea-salt particles were completely depleted Cl and contained excessive S due to the influence of polluted air masses derived from the Asian continent.

(5) Approximately 30% of modified sea-salt particles had diameters larger than 2.0 μm, whereas most sulfates had diameters less than 2.0 μm. Their gravitational deposition velocities suggested that if the acidic substances react with sea-salt particles, their lifetime in the atmosphere shortens due to dry deposition, implying the importance of the scavenging effect of sea-salt particles for Earth's radiation budget.

We found that sea-salt particles and sulfate dominated the aerosol particles over the open ocean. These particles also interact with each other, forming modified sea-salt particles at the individual particle scale. The sources of sulfur varied widely, including anthropogenic, volcanic, and biological activities, depending on location and air mass history. The sizes of particles reflect their transport history, and eventually affect their atmospheric lifetime. These results show that, although the marine aerosol particles were collected far from continents and anthropogenic sources, they still change their compositions at the individual scale with age. Therefore, if it was assumed that they were just sodium chloride particles, their influences on the climate would not be accurately evaluated; the consideration of their modification processes is important for marine aerosol particles.

Acknowledgements This study was supported by funds from the Ministry of Education, Culture, Sports, Science and Technology, Japan; Grant-Aid for Scientific Research on Innovative Areas "New Ocean Paradigm on Its Biogeochemistry, Ecosystem and Sustainable Use (NEOPS)" under Grant No. 25121504. This study was also supported by the Research Fund of Tokyo University of Science, Japan. We are grateful to the captains and crews of the R/V Hakuho Maru of KH-13-7 and KH-14-3 cruises, principal researcher Dr. H. Ogawa (The University of Tokyo), Dr. A. Tsuda (The University of Tokyo), Dr. M. Sato (The University of Tokyo) and other researchers for their support with onboard aerosol measurements. We are also grateful to Dr. H. Furutani and Mr. Y. Miki for sampling aerosol particles during the KH-13-7 cruise, and Mr. S. Yokoyama for analyzing the radon data during both cruises. We appreciate Dr. K. Hara (Fukuoka University), Dr. I. Hashimoto (Tokyo University of Science) and Dr. Y. Narita (Atmosphere and Ocean Research Institute, The University of Tokyo) for their helpful comments.

Appendix

See Fig. 9.

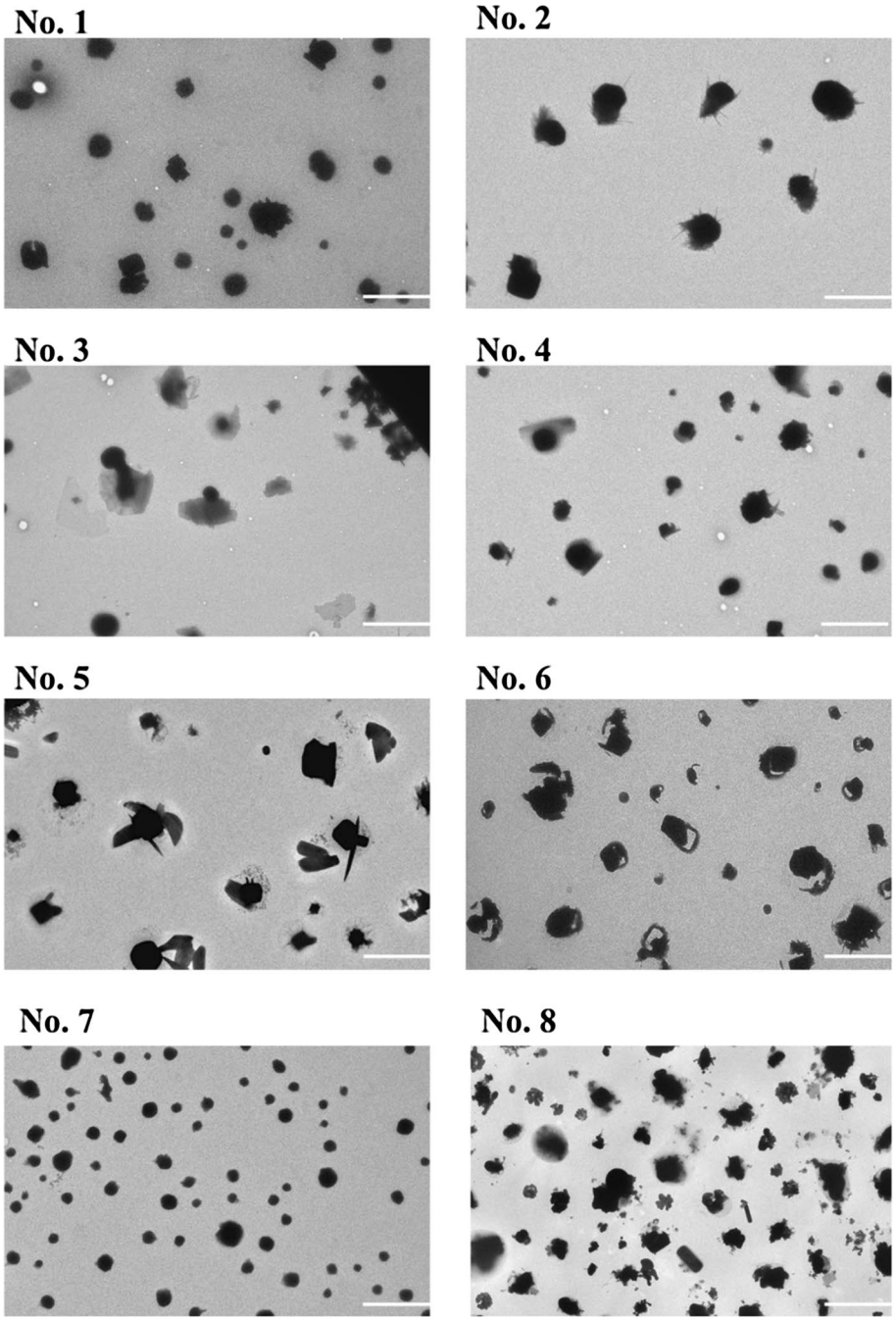

Fig. 9 TEM images of each sample. A white line is a scale bar of 5 μm

References

Adachi K, Buseck PR (2015) Changes in shape and composition of sea-salt particles upon aging in an urban atmosphere. Atmos Chem 100:1–9. https://doi.org/10.1016/j.atmosenv.2014.10.036

Berresheim H, Eisele FL, Tanner DJ, Mclnnes LM, Ramsey-Bell DC, Covert DS (1993) Atmospheric sulfur chemistry and cloud condensation nuclei (CCN) concentrations over the northeastern Pacific Coast. J Geophys Res Atmos 98(D7):12701–12711. https://doi.org/10.1029/93JD00815

Chi JW, Li WJ, Zhang DZ, Zhang JC, Lin YT, Shen XJ, Sun JY, Chen JM, Zhang XY, Zhang YM, Wang WX (2015) Sea salt aerosols as a reactive surface for inorganic and organic acidic gases in the Arctic troposphere. Atmos Chem Phys 15:11341–11353. https://doi.org/10.5194/acp-15-11341-2015

Furutani H, Jung J, Miura K, Takami A, Kato S, Kaji Y, Uematsu M (2011) Single-particle chemical characterization and source apportionment of iron-containing atmospheric aerosols in Asian outflow. J Geophys Res 116:D18204. https://doi.org/10.1029/2011JD015867

Gong SL, Barrie LA (2003) Simulating the impact of sea salt on global nss sulphate aerosols. J Geophys Res Atmos 108(D16):4516. https://doi.org/10.1029/2002JD003181

Hara K, Osada K, Kido M, Matsunaga K, Iwasaka Y, Hashida G, Yamanouchi T (2005) Variations of constituents of individual

sea-salt particles at Syowa station, Antarctica. Tellus B 57(3):230–246. https://doi.org/10.3402/tellusb.v57i3.16530

Hara K, Osada K, Yamanouchi T (2013) Tethered balloon-borne aerosol measurements: seasonal and vertical variations of aerosol constituents over Syowa Station, Antarctica. Atmos Chem Phys 13:9119–9139. https://doi.org/10.5194/acp-13-9119-2013

IPCC (2013) IPCC(AR5): climate change 2013: the physical science basis, summary for policymakers, contribution of working group to the fifth assesment report. IPCC, Switzerland

Kasten F (1968) Falling speed of aerosol particles. J Appl Meteorol 7(5):944–947. https://doi.org/10.1175/1520-0450(1968)007%3c0944:FSOAP%3e2.0.CO;2

Laskin A, Moffet RC, Gilles MK, Fast JD, Zaveri RA, Wang B, Nigge P, Shutthanandan J (2012) Tropospheric chemistry of internally mixed sea salt and organic particles: surprising reactivity of NaCl with weak organic acids. J Geophys Res 117:D15302. https://doi.org/10.1029/2012JD017743

LeGrande AN, Tsigaridis K, Bauer SE (2016) Role of atmospheric chemistry in the climate impacts of stratospheric volcanic injections. Nat Geosci 9:652–655. https://doi.org/10.1038/ngeo2771

Li W, Shao L, Shen R, Yang S, Wang Z, Tang U (2011) Internally mixed sea salt, soot, and sulfates at Macao, a coastal city in South China. J Air Waste Manag Assoc 61:1166–1173. https://doi.org/10.1080/10473289.2011.603996

Li W, Xu L, Liu X, Zhang J, Lin Y, Yao X, Gao H, Zhang D, Chen J, Wang W, Harrison RM, Zhang X, Shao L, Fu P, Nenes A, Shi Z (2017) Air pollution-aerosol interactions produce more bioavailable iron for ocean ecosystems. Sci Adv 3(3):e1601749. https://doi.org/10.1126/sciadv.1601749

Matsui H, Mahowald NM, Moteki N, Hamilton DS, Ohata S, Yoshida A, Koike M, Scanza RA, Flanner MG (2018) Anthropogenic combustion iron as a complex climate forcer. Nat Commun 9(1):1593. https://doi.org/10.1038/s41467-018-03997-0

Miura K (2000) Physical and chemical properties of aerosols in the marine boundary layer. Earozoru Kenkyu 15(4):327–334. https://doi.org/10.11203/jar.15.327 **(in Japanese)**

Miura K, Kumakura T, Sekikawa T (1991) The effect of continental air mass on the modification of individual sea-salt particles collected over the coast and the open sea. J Meteorol Soc Jpn Ser II 69(4):429–438. https://doi.org/10.2151/jmsj1965.69.4_429

Mouri H, Okada K (1993) Shattering and modification of sea-salt particles in the marine atmosphere. Geophys Res Lett 20(1):49–52. https://doi.org/10.1029/92GL03004

Mouri H, Okada K, Takahashi S (1995) Giant sulfur-dominant particles in remote marine boundary layer. Geophys Res Lett 22(5):595–598. https://doi.org/10.1029/94GL03394

Mouri H, Nagao I, Okada K, Koga S, Tanaka H (1996) Elemental composition of individual aerosol particles collected from the coastal marine boundary layer. J Meteorol Soc Jpn Ser II 74(5):585–591. https://doi.org/10.2151/jmsj1965.74.5_585

Mouri H, Nagao I, Okada K, Koga S, Tanaka H (1999) Individual-particle analyses of coastal Antarctic aerosols. Tellus B 51(3):603–611. https://doi.org/10.3402/tellusb.v51i3.1644

Ooki A, Miura K, Uematsu M (2003) The increase of biogenic sulfate aerosol and particle number in marine atmosphere over the Northwestern North Pacific. J Oceanogr 59(6):799–807. https://doi.org/10.1023/B:JOCE.0000009571.81193.5d

Rolph G, Stein A, Stunder B (2017) Real-time environmental applications and display system: READY. Environ Model Softw 95:210–228. https://doi.org/10.1016/j.envsoft.2017.06.025

Seinfeld JH, Pandis SN (2016) Atmospheric chemistry and physics: from air pollution to climate change. John Wiley & Sons, Hoboken

Stein AF, Draxler RR, Rolph GD, Stunder BJB, Cohen MD, Ngan F (2015) NOAA's HYSPLIT atmospheric transport and dispersion modeling system. Bull Am Meteorol Soc 96(12):2059–2077. https://doi.org/10.1175/BAMS-D-14-00110.1

Tomimatsu M, Miura K, Ueda S, Furutani H, Uematsu M (2012) Properties of individual aerosol particles collected over the East Philippines Ocean. Proc Soc Atmos Electr Jpn 6(1):170–171 **(in Japanese)**

U.S. Standard Atmosphere (1976) U.S. Government Printing Office, Washington, D.C

Volcano Discovery. http://www.volcanodiscovery.com. Accessed 1 Nov 2017